Negative permittivity and permeability in the infrared due to dielectric spheres

Mark S. Wheeler, J. Stewart Aitchison, and Mohammad Mojahedi

The Edward S. Rogers Sr. Department of Electrical and Computer Engineering
University of Toronto
10 King's College Road, Toronto, Ontario, M5S 3G4, Canada

ABSTRACT

In this paper we consider the effective electric and magnetic properties of a three-dimensional collection of non-magnetic spheres. Polaritonic materials are used, so that the Mie resonances of the spheres are excited in the long-wavelength regime of the surrounding medium. We consider a simple cubic lattice based on $LiTaO_3$ and find that it is possible to engineer a fundamental resonant magnetic response. The effective media parameters derived by this approach are isotropic, and closely match those obtained by band structure calculations. Frequency ranges with either negative permittivity or negative permeability are found. Within these ranges a negative group velocity is observed. Coated spheres with a negative index of refraction are also presented.

Keywords: Metamaterials, Mie scattering, magnetism, negative permeability, negative permittivity, negative index of refraction, negative group velocity

1. INTRODUCTION

The research into negative index of refraction metamaterials has progressed rapidly within the past few years. The investigations of artificial materials with either a negative permittivity at frequencies below the ultraviolet,[1] or with a magnetic response or negative permeability above the megahertz range,[2] stimulated interest in the possibility that materials with a negative refraction could be synthesized. The combination of the two aforementioned types of metamaterials was subsequently found to have a negative index of refraction.[3] The first potential application, the perfect lens,[4] promised that a planar slab of such material could focus both the propagating and evanescent components of an object and achieve sub-wavelength imaging, and great excitement spawned this new field of research. Since then, a negative index has also been demonstrated in loaded transmission line media,[5] and a related effect has been found to occur in photonic crystals.[6,7] Experimental results have been reported in the GHz range for Snell's law.[8]

The bulk of the investigations in metamaterials have been limited to the microwave domain, since there has been considerable difficulty in pushing the results to infrared and optical frequencies due to the need for a strong magnetic response at these frequencies. Even though the structures used can be scaled down in principle, the intricate features of the materials which provide the magnetic response, such as the split-ring resonators,[2] are not simple to fabricate, and they are made of metals which are lossy at infrared frequencies. In addition, the split-ring resonators are inherently anisotropic, and a complex arrangement of them would be needed to make an isotropic composite. We propose an alternate structure which can provide a negative permeability and also a negative permittivity.

On the other hand, photonic crystal designs[6,7] may be simpler structures, but it is the Bragg scattereing in high-order bands, and not the long-wavelength effective media values, which causes the negative refraction effect. This leads to a number of practical difficulties with the photonic crystals such as anisotropy, mode coupling mismatches, and high-order diffraction.[7] In addition, the fact that the wavelength is on the order the lattice constant means that these PCs are limited in their use in device miniaturization. Furthermore, the transmission line media are also unsuitable at the infrared frequencies due to their lumped components or intricate printed loading elements.

Further author information: E-mail: mark.wheeler@utoronto.ca

There have been reports on structures with a negative effective permeability, which could replace the split-ring resonantors. It has been reported[10] that a two-dimensional array of ferroelectric rods can have a negative effective permeability in the GHz range when the magnetic field is polarized along the axes of the rods. The rods, composed of materials with a large dielectric constant, act as leaky resonant cavities in the long-wavelength limit, with the displacement currents circulating around each rod. These displacement currents are equivalent to magnetic dipoles, and the resulting strong resonant behaviour was then averaged to find a negative effective permeability. It was subsequently shown that polaritonic rods can also be used to extend this concept to the infrared in two dimensions.[11]

Here we report that a three-dimensional collection of polaritonic *spheres* can have a negative effective permeability in the infrared.[12] In addition, this effective permeability is found to be isotropic for modest filling fractions. The effective electromagnetic constants are derived by a simple and rigorous method. The effective permeability and permittivity are obtained in the long-wavelength limit, which only depend on the dielectric permittivity of the constituent spheres and their volume filling fraction. Both the effective permittivity and permeability can be negative, although not at the same frequency. The effective medium theory and the isotropy of the composite are verified by a numerical scattering matrix method. Finally, scattering by coated spheres is shown to result in a composite with a negative index of refraction.

2. EFFECTIVE MEDIUM APPROACH

The scattering problem of a single dielectric sphere is now considered. The scattered field is compared to the standard form of dipole radiation, and the dipole moments are derived. The effective polarizabilities are then used with the Clausius-Mossotti relation to find the effective electromagnetic parameters. Since the permeability is of particular interest, the derivation follows the magnetic fields, and the dual relations hold for the electric fields.

A plane wave with wavevector $\mathbf{k}_0 = \omega\hat{\mathbf{z}}/c$ and magnetic field $\mathbf{H}_i = H_0 \exp(ik_0 z)\hat{\mathbf{y}}$ is incident on a single isolated sphere of radius r_0 and relative permittivity $\epsilon_r = n^2$. The constants of proportionality between the 2^m-multipole terms of the magnetic field scattered by the sphere and those of the incident field are

$$b_m = \frac{\psi_m(nx)\psi'_m(x) - n\psi_m(x)\psi'_m(nx)}{\psi_m(nx)\xi'_m(x) - n\xi_m(x)\psi'_m(nx)}, \tag{1}$$

and the 2^m-pole coefficients of the scattered electric field are

$$a_m = \frac{n\psi_m(nx)\psi'_m(x) - \psi_m(x)\psi'_m(nx)}{n\psi_m(nx)\xi'_m(x) - \xi_m(x)\psi'_m(nx)}. \tag{2}$$

Here $x = k_0 r_0$, and $\psi_m(z) = z j_m(z)$ and $\xi_m(z) = z h^1_m(z)$ are the Riccati-Bessel functions, which are related to the spherical Bessel and spherical Hankel functions.[13] The primes indicate differentiation with respect to the argument.

The dipole scattered fields, *i.e.* those with $m = 1$, are of interest here. Only the b_1 coefficient, which is the strength of the magnetic dipole response, is needed when considering the effective permeability, while only the a_1 term is needed to find the effective permittivity.

The forms of a_m and b_m show that they can have a resonant response. Therefore, consider a situation where the frequency of the incident wave is such that only one of these terms is dominant; *e.g.* b_1 is near resonance. The dominant contribution to the scattered magnetic field is then due to the single term,

$$\begin{aligned}\mathbf{H}^{\mathbf{ff}} &= \frac{3i}{2} H_0 b_1 \frac{e^{ik_0 r}}{k_0 r}\left[\left(\hat{\mathbf{y}}\cdot\hat{\boldsymbol{\theta}}\right)\hat{\boldsymbol{\theta}} + \left(\hat{\mathbf{y}}\cdot\hat{\boldsymbol{\varphi}}\right)\hat{\boldsymbol{\varphi}}\right] \\ &= -\frac{3i}{2} H_0 b_1 \frac{e^{ik_0 r}}{k_0 r}\hat{\mathbf{r}}\times\left(\hat{\mathbf{r}}\times\hat{\mathbf{y}}\right),\end{aligned} \tag{3}$$

in the far-field.[13] If the free-space wavelength is much larger than the diameter of the sphere, the sphere may be replaced conceptually by a radiating magnetic dipole of moment $\mathbf{m}$. The scattered field may then be compared to the standard expression for far-field dipole radiation,[14]

$$\mathbf{H^{ff}} = -\frac{k_0^3}{4\pi}\frac{e^{ik_0 r}}{k_0 r}\hat{\mathbf{r}} \times (\hat{\mathbf{r}} \times \mathbf{m}) \,. \tag{4}$$

The equivalent magnetic dipole moment of a single isolated dielectric sphere may be then found by equating (3) and (4), in terms of its b_1 scattering coefficient,[15]

$$\mathbf{m} = 6\pi i H_0 b_1 \hat{\mathbf{z}}/k_0^3. \tag{5}$$

The effective magnetic polarizability α_m can then be found, where $\mathbf{m} = \alpha_m \mathbf{H}_i$, which yields

$$\alpha_m = 6\pi i b_1/k_0^3. \tag{6}$$

Therefore, the dielectric sphere can be removed and replaced by an ideal dipole of effective moment $\mathbf{m}$ and effective polarizability α_m.

In order to describe the response of a bulk material (a large collection of spheres), the effective permeability μ_r^{eff} is needed. This can be found by averaging the effective dipole fields over a large region in the long-wavelength limit. The results, known as the Clausius-Mossotti equation,[14] or the Lorentz-Lorenz formula,[16] can be used to relate the bulk effective permeability to the single sphere polarizability,

$$\alpha_m = \frac{3}{N}\left(\frac{\mu_r^{\text{eff}} - 1}{\mu_r^{\text{eff}} + 2}\right), \tag{7}$$

where N is the sphere volume density. The filling fraction f of the composite is $f = 4\pi N r_0^3/3$, and should be kept to modest values. The effective permeability is then

$$\mu_r^{\text{eff}} = \frac{k_0^3 + 4\pi i N b_1}{k_0^3 - 2\pi i N b_1}. \tag{8}$$

Similarly, the effective permittivity ϵ_r^{eff} can be related to the scattered electric dipole term a_1,

$$\epsilon_r^{\text{eff}} = \frac{k_0^3 + 4\pi i N a_1}{k_0^3 - 2\pi i N a_1}. \tag{9}$$

These two final expressions determine the response of the bulk composite, and depend only on the size, density, and composition of the spheres.

3. NEGATIVE PERMEABILITY

The magnetic dipole response of a sphere is usually weak. In addition, even though the coefficient b_1 resonates due to the spherical Bessel functions, these resonances are often at frequencies beyond the long-wavelength limit and thus are not valid in the bulk μ_r^{eff}. This applies in most circumstances, when the materials that comprise the sphere are dielectrics or metals. However, if the material dielectric constant were very large, the magnetic response coefficient b_1 could be driven into resonance at very low frequencies, within the long-wavelength limit. Some classes of materials that can provide the large dielectric constant are ferroelectric or polaritonic materials. These materials were considered in the reports of the related magnetic resonances in two-dimensional arrays of dielectric cylinders.[10,11] Whereas ferroelectrics may be more useful in the microwave range, the lattice resonance (*reststrahl* region) in polaritonic crystals can be exploited at infrared and optical frequencies, and is considered in this paper.

The relative permittivity of polaritonic materials follows the relation

$$\epsilon_r(\omega) = \epsilon(\infty)\left(1 + \frac{\omega_L^2 - \omega_T^2}{\omega_T^2 - \omega^2 - i\omega\gamma}\right), \tag{10}$$

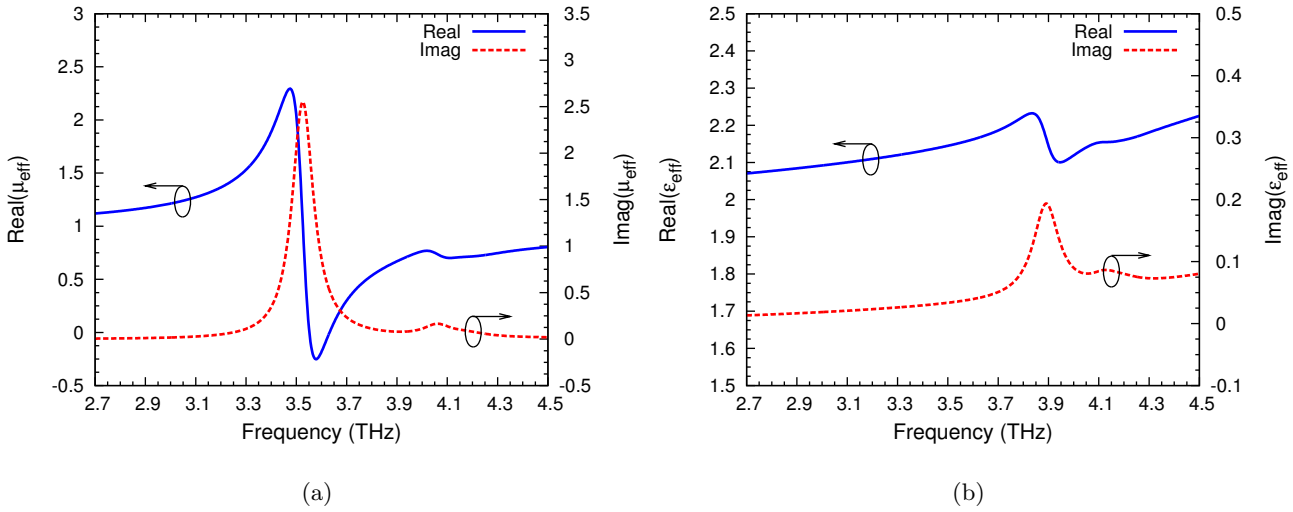

(a) (b)

Figure 1. The effective relative (a) permeability and (b) permittivity of a collection of $LiTaO_3$ spheres. The radius of the spheres is $4\,\mu$m. The filling fraction is 26.81%.

where $\epsilon(\infty)$ is the high-frequency limit of the permittivity, ω_T is the transverse optical phonon frequency, ω_L is the longitudinal optical phonon frequency, and γ is the damping coefficient.[17] These parameters are related by the Lyddane-Sachs-Teller relation $\omega_L^2/\omega_T^2 = \epsilon(0)/\epsilon(\infty)$, where $\epsilon(0)$ is the static permittivity. We consider spheres made of $LiTaO_3$, and use the following parameters[18]: $\epsilon(0) = 41.4$, $\epsilon(\infty) = 13.4$, $\omega_T = 2\pi \times 4.25 \times 10^{12}$ rad/s, $\omega_L = 2\pi \times 7.46 \times 10^{12}$ rad/s, and $\gamma = 2\pi \times 1.5 \times 10^{11}$ rad/s.

We have chosen $LiTaO_3$ because of its large static permittivity $\epsilon(0)$. The permittivity increases with frequency up to the transverse phonon frequency ω_T, where it is extremely large. It is just below this material resonance that the permittivity becomes sufficiently large to drive the magnetic dipole into resonance. That is, the large dielectric constant, and not necessarily the material resonance, is the desired attribute of polaritonic materials; the larger the permittivity, the easier it is to create a negative effective permeability.

We consider a collection of $LiTaO_3$ spheres, with filling fraction 26.81% and radii $4\,\mu$m. The effective permeability is shown in Fig. 1(a), and the effective permittivity is shown in Fig. 1(b). The frequency ranges shown are within the long-wavelength limit; the ratio of the free-space wavelength to the diameter of the sphere at the center of the permeability resonance is 10.6.

The resonance in $\mu_r^{\rm eff}$ shown in Fig. 1(a) is centered at 3.53 THz, which is slightly below the transverse phonon frequency ($\omega_T = 4.25$ THz), but nevertheless the material permittivity is quite large. The values of $\mu_r^{\rm eff}$, which are otherwise assumed to be unity at optical frequencies, vary substantially from that. A negative permeability is shown above the resonance. There is not much structure in $\epsilon_r^{\rm eff}$, shown in Fig. 1(b), other than a very weak resonance at 3.9 THz.

Finally, we note that the effective medium approach presented here differs from the method commonly used on other metamaterials.[10] In the other method, the effective index and effective impedance are transformed into the effective permeability and permittivity. The effective index is found from band structure calculations. The effective impedance is derived from the equivalence in reflection from a slab of some thickness of the metamaterial, and the same length of a homogeneous slab. The slab thickness is arbitrary, and the resulting effective media values are implicitly dependent on it. A number of reports that use this other method find negative imaginary values of either the permittivity or permeability,[10, 11, 19] which indicate that the passive structures have gain, which is unsettling. On the other hand, the method presented here is a first-principles approach, and as shown in Fig. 1, the imaginary parts are always non-negative, indicating attenuation only, as should be expected.

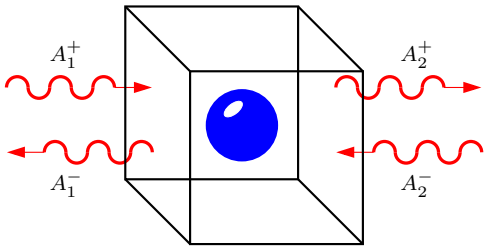

Figure 2. A unit cell of a simple cubic crystal, indicating the components of the scattered waves. This figure assumes propagation along the ΓX direction.

4. BAND STRUCTURE AND ISOTROPY

The effective values presented in Sect. 3 were calculated only knowing the density of the collection of spheres. The actual arrangement of the spheres, particularly a periodic lattice arrangement, should make little difference on the band structure, since the wavelengths are much larger than the spheres or their spacing. Therefore, the effective media values are expected to be isotropic. A full numerical calculation, which takes into account the multiple scattering between the spheres in a lattice, is desired to verify that the dispersion is the same in all directions. This would also include the higher multipole contributions. Therefore, we will compare the effective medium results with photonic crystal band structure calculations. In addition, this will verify the accuracy of the calculated effective medium values.

We used modifications of the code MULTEM2 to perform the band structure calculations.[20] A three-dimensional array of spheres is partitioned into a stack of two-dimensional planes of spheres, perpendicular to the direction of wave propagation. A scattering matrix approach relates the fields on the two ends of a unit cell along the direction of propagation,

$$\begin{aligned} \mathbf{A}_2^+ &= \mathbf{T}_{21} \cdot \mathbf{A}_1^+ + \mathbf{R}_{22} \cdot \mathbf{A}_2^- \\ \mathbf{A}_1^- &= \mathbf{R}_{11} \cdot \mathbf{A}_1^+ + \mathbf{T}_{12} \cdot \mathbf{A}_2^-, \end{aligned} \tag{11}$$

where $\mathbf{A}_i^{\pm}$ are column vectors representing the components of the fields, as defined in Fig. 2. The $\mathbf{T}_{ij}$ and $\mathbf{R}_{ij}$ are transmission and reflection matrices from the j-th to i-th plane, and include all of the information regarding the lattice, sphere size, sphere and host dielectrics, frequency, and transverse wavevector. The Bloch condition is imposed along the direction of propagation, so that $\mathbf{A}_2^{\pm} = \exp(ika)\mathbf{A}_1^{\pm}$, where k is the longitudinal component of the Bloch wavevector, and a is the unit cell size. The code then solves the eigenvalue problem

$$e^{ika} \begin{bmatrix} \mathbf{I} & \mathbf{0} \\ \mathbf{R}_{11} & \mathbf{T}_{12} \end{bmatrix} \begin{bmatrix} \mathbf{A}_1^+ \\ \mathbf{A}_2^- \end{bmatrix} = \begin{bmatrix} \mathbf{T}_{21} & \mathbf{R}_{22} \\ \mathbf{0} & \mathbf{I} \end{bmatrix} \begin{bmatrix} \mathbf{A}_1^+ \\ \mathbf{A}_2^- \end{bmatrix}, \tag{12}$$

where $\mathbf{I}$ is the identity matrix. The only approximations in this code are in the angular momentum cutoff in the spherical scattering coefficients, and the number of reciprocal lattice vectors taken in each two-dimensional plane of spheres. The code was modified from the published version[20] to accommodate polaritonic materials.

A simple cubic lattice is chosen to verify the effective medium approach and isotropy. The lattice constant is $a = 10\,\mu$m, and the $LiTaO_3$ spheres have a radius of $r_0 = 0.4a$. This is a filling fraction of 26.81% (using $N = 1/a^3$ for a simple cubic lattice), which corresponds to the values used in the effective medium approach in Sect. 3. The band structures calculated with the scattering matrix code for the Bloch wavevector along the ΓX, ΓM, and ΓR directions are shown in Fig. 3(a). These are compared with the effective photon dispersion, which is given by the relation

$$c^2 k_0^2 = \omega^2 \epsilon_r^{\text{eff}}(\omega) \mu_r^{\text{eff}}(\omega), \tag{13}$$

in the long-wavelength limit, where $\mu_r^{\text{eff}}(\omega)$ and $\epsilon_r^{\text{eff}}(\omega)$ were obtained from (8) and (9). All of the curves match closely, verifying both the effective medium approach as well as the isotropic response of the composite. Note that the ΓM direction should have two non-degenerate bands, which can be distinguished in Fig. 3(a), although for one of these bands the code did not converge easily at the center of the resonance. The long-wavelength

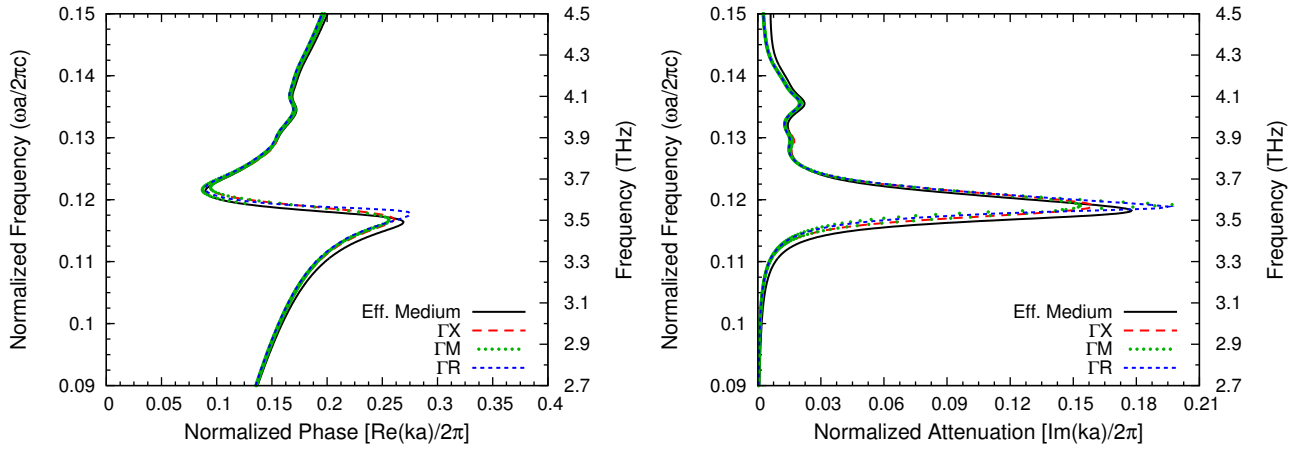

Figure 3. The eigenfrequencies of a simple cubic lattice of $LiTaO_3$ spheres, as a function of the (a) real part (band structure), and (b) imaginary part of the Bloch wavevector. The lattice constant is $a = 10\,\mu$m and the radius of the spheres is $r_0 = 0.4a$.

approximation begins to break down at frequencies slightly beyond the range of the figure, most noticably near the first Bragg gap (around $ka/2\pi = 0.5$ and $\omega a/2\pi c = 0.35$), which is a feature that cannot be predicted by the effective medium approach, and is beyond its limits of validity.

The most interesting feature of the band structure is the "kink" centered at $\omega a/2\pi c = 0.118$. This is due to the resonance in the effective permeability. This is an anomalous dispersion region that has a negative group velocity, $v_g = \partial\omega/\partial k < 0$. A negative group velocity means that the group delay of a pulse traveling through the structure is negative. That is, if a pulse in this frequency range were applied to a slab of this material, the peak output would *precede* the input peak. This does not violate causality, so long as the passive media displays attenuation in the anomalous dispersion region.[5, 21] As such, the attenuation is proportional to the imaginary part of the Bloch wavevector, which is shown in Fig. 3(b). This manifests itself as a pseudogap, meaning that the phase varies throughout the width of the gap, in contrast to the constant phase in the Bragg gap.

5. NEGATIVE PERMITTIVITY

Now we would like to discuss how to design significant values of ϵ_r^{eff}, particularly negative values. The effective permittivity was derived in Eq. (9). As such, resonances of a_1 are manifested as bulk resonances in ϵ_r^{eff}. However, the same concept of using large-valued dielectric materials to drive these resonances does not apply as simply as before, since the fundamental resonance of a_1 is above that of b_1. Since these resonances must be kept in the range of $\lambda_0/a \gtrsim 10$, it is more difficult to use these bulk resonances to synthesize a negative permittivity.

There exists another way to induce a resonance in ϵ_r^{eff}. Relaxing the condition that the sphere material must be a large dielectric, the electric scattering coefficient can be approximated as[13]

$$a_1 = -\frac{i2x^3}{3}\frac{\epsilon_r - 1}{\epsilon_r + 2}, \qquad |\sqrt{\epsilon_r}|x \ll 1. \tag{14}$$

Therefore, an isolated sphere will have a resonance in a_1 if $\epsilon_r = -2$. Using Eq. (14) in Eq. (9), we find that

$$\epsilon_r = \frac{f+2}{f-1} \tag{15}$$

is an approximate condition for the material permittivity of the sphere that induces a resonance in ϵ_r^{eff}. The required material permittivity will always be negative, and grows more negative with increasing filling fraction.

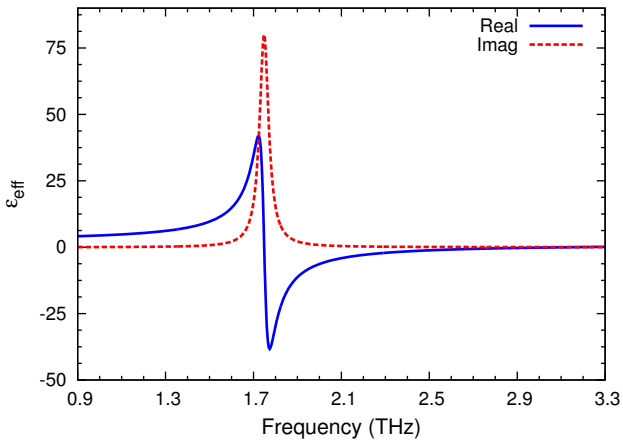

Figure 4. The effective permittivity of a simple cubic arrangement of spheres. The lattice constant is $a = 10\,\mu$m, the sphere radius is $r_0 = 0.47a$, and the spheres are made of a Drude material with $\omega_p = 25.8$ THz and $\gamma = \omega_p/100$.

As such, this is a surface resonance, and the radial dependence of the field decays (with modified spherical Bessel functional form) into the sphere.

Now consider spheres made of a material represented by a Drude model,

$$\epsilon(\omega) = 1 - \frac{\omega_p^2}{\omega^2 + i\omega\gamma}, \tag{16}$$

with plasma frequency ω_p and damping term γ. This model describes metals and semiconductors, and (15) indicates that we are concerned with the small negative values of permittivity that are obtained at frequencies just below ω_p. Since we are considering frequencies in the THz range, metals are excluded, due to their typical ultraviolet plasma frequencies. We therefore consider semiconductor materials, and use parameters of $\omega_p = 25.8$ THz and $\gamma = \omega_p/100$, which could be achieved with proper doping. The radius of each sphere is $r_0 = 0.47a$. Using (15) and (16), the resonance in ϵ_r^{eff} is expected to be at 1.78 THz, where the sphere permittivity is $\epsilon = -4.31 + i0.13$. The calculated ϵ_r^{eff} is shown in Fig. 4. The values for μ_r^{eff} do not vary significantly from unity, and are not shown.

6. NEGATIVE INDEX OF REFRACTION

A negative index of refraction requires both a negative permeability and permittivity at the same frequency. Section 3 described how to design a negative permeability, and Sect. 5 described how to design a negative permittivity. Unfortunately, one cannot design *both* to be negative in the same frequency range with the present model. Nevertheless, the same concepts can be applied to more complex structures. One method, reported very recently,[22] uses two interpenetrating arrays of spheres; one set is tuned to have $\mu_r^{\text{eff}} < 0$, and the other is tuned to have $\epsilon_r^{\text{eff}} < 0$.

Here we report another possibility: using coated spheres. In particular, we choose to tune the core to have $\mu_r^{\text{eff}} < 0$, and the shell to have $\epsilon_r^{\text{eff}} < 0$. Consider now a core, of radius r_1 and index $n_1 = \epsilon_1^2$, coated by a shell of radius r_2 (measured from the same origin) and index $n_2 = \epsilon_2^2$. Then the scattering coefficients, in place of (1)

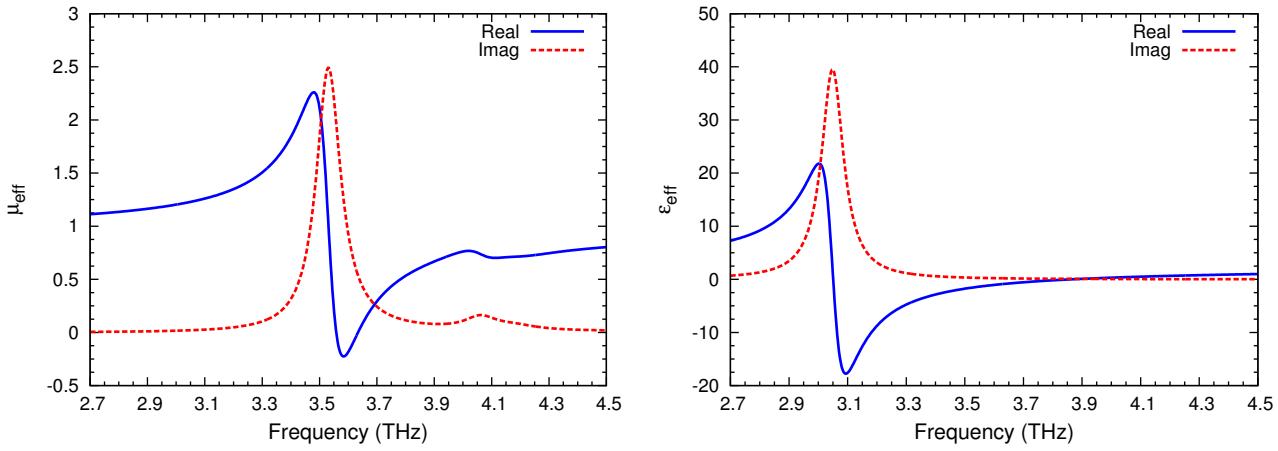

(a) (b)

Figure 5. The (a) effective permeability and (b) effective permittivity of a simple cubic lattice of coated spheres. The lattice constant is $a = 10\,\mu$m. The cores are $LiTaO_3$ spheres of radius $r_1 = 0.4a$, and the shells are a Drude material with $r_2 = 0.47a$, $\omega_p = 25.8$ THz and $\gamma = \omega_p/100$.

and (2) are,[13]

$$a_m = \frac{\psi_m(y)\left[\psi_m'(n_2y) - A_m\chi_m'(n_2y)\right] - n_2\psi_m'(y)\left[\psi_m(n_2y) - A_m\chi_m(n_2y)\right]}{\xi_m(y)\left[\psi_m'(n_2y) - A_m\chi_m'(n_2y)\right] - n_2\xi_m'(y)\left[\psi_m(n_2y) - A_m\chi_m(n_2y)\right]}, \tag{17}$$

$$b_m = \frac{n_2\psi_m(y)\left[\psi_m'(n_2y) - B_m\chi_m'(n_2y)\right] - \psi_m'(y)\left[\psi_m(n_2y) - B_m\chi_m(n_2y)\right]}{n_2\xi_m(y)\left[\psi_m'(n_2y) - B_m\chi_m'(n_2y)\right] - \xi_m'(y)\left[\psi_m(n_2y) - B_m\chi_m(n_2y)\right]}, \tag{18}$$

$$A_m = \frac{n_2\psi_m(n_2x)\psi_m'(n_1x) - n_1\psi_m'(n_2x)\psi_m(n_1x)}{n_2\chi_m(n_2x)\psi_m'(n_1x) - n_1\chi_m'(n_2x)\psi_m(n_1x)}, \tag{19}$$

$$B_m = \frac{n_2\psi_m(n_1x)\psi_m'(n_2x) - n_1\psi_m(n_2x)\psi_m'(n_1x)}{n_2\chi_m'(n_2x)\psi_m(n_1x) - n_1\psi_m'(n_1x)\chi_m(n_2x)}, \tag{20}$$

where $x = kr_1$, $y = kr_2$, $\chi_m(z) = -zy_m(z)$, and $y_m(z)$ is the spherical Bessel function of the second kind. To find the effective media values for coated spheres, one simply uses these equations in (8) and (9).

Our heuristic for tailoring $\mu_r^{\text{eff}} < 0$ was to use fairly large spheres with a large material permittivity. We choose to use the example design in Sect. 3 again as the core. This will provide the necessary $\mu_r^{\text{eff}} < 0$ and we shall choose a shell that will not interact in terms of its magnetic response. The design of the shell is not simple, since both the core and the shell will contribute to the electric response. Nevertheless, by using the Drude sphere presented in Sect. 5, and carving out the center volume equal to the volume of the $LiTaO_3$ core, a negative index design is achieved. The resulting effective media values are shown in Fig. 5. Note that the regions of $\mu_r^{\text{eff}} < 0$ and $\epsilon_r^{\text{eff}} < 0$ overlap in frequency. The permittivity resonance has shifted up in frequency because the effective filling fraction of the Drude shell (surface wave evanescent region) has been lowered.

Finally, the effective index of these coated spheres, calculated with $n_{\text{eff}} = \sqrt{\mu_r^{\text{eff}}}\sqrt{\epsilon_r^{\text{eff}}}$, in shown in Fig. 6(a), and the band structure, calculated from (13), is shown in Fig. 6(b). There is a band of frequencies where the real part of the index is negative. The imaginary part of the index, which is proportional to attenuation, has moderate values in this range, and is primarily a consequence of the attenuation of the effective permeability

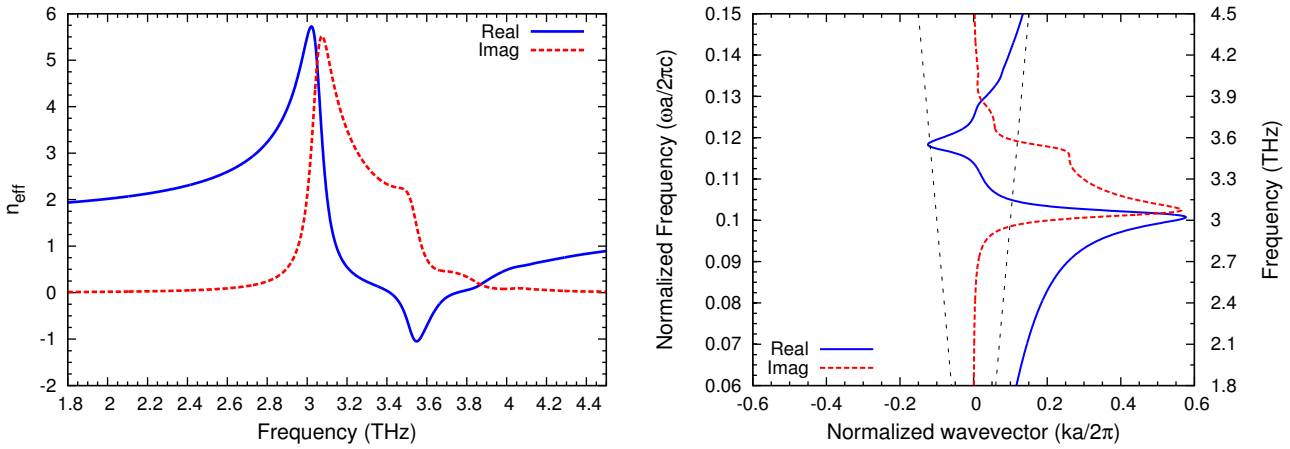

(a) (b)

Figure 6. The (a) effective index and (b) band structure of a simple cubic lattice of coated spheres. The structure is the same as in Fig. 5.

resonance. Both resonances can be seen in the band structure, and the real part of the curve crosses into a range where $k < 0$. The negative index region can be found in the band structure where $k < 0$ and $d\omega/dk > 0$, *i.e.* $v_p < 0$ and $v_g > 0$, which are the characteristics of negative index and backward wave behaviour.

7. SUMMARY

A first-principles approach for calculating the effective permeability and permittivity of a collection of dielectric spheres has been presented. It has been shown that a collection of polaritonic spheres can have an effective permeability that differs substantially from unity at infrared frequencies, and can even be negative. The three-dimensional isotropic magnetic response is controlled by the size, density, and dielectric properties of the spheres. This composite is a simple alternative to the use of split ring resonator in optical metamaterials. Furthermore, designs with a negative effective permittivity and negative index of refraction were also reported. This work shows that simple spheres can be used to make metamaterials in the optical domain.

This work was supported by the Natural Sciences and Engineering Research Council of Canada under Grant No. 249531-02, and in part by Photonic Research Ontario, Funded Research No. 72022792.

REFERENCES

1. J. B. Pendry, A. J. Holden, W. J. Stewart, and I. Youngs, "Extremely low frequency plasmons in metallic mesostructures," *Phys. Rev. Lett.* **76**, pp. 4773–4776, 1996.
2. J. B. Pendry, A. J. Holden, D. J. Robbins, and W. J. Stewart, "Magnetism from conductors and enhanced nonlinear phenomena," *IEEE Trans. Microwave Theory Tech.* **47**(11), pp. 2075–2084, 1999.
3. D. R. Smith, W. J. Padilla, D. C. Vier, S. C. Nemat-Nasser, and S. Schultz, "Composite medium with simultaneously negative permeability and permittivity," *Phys. Rev. Lett.* **84**, p. 4184, 2000.
4. J. B. Pendry, "Negative refraction make a perfect lens," *Phys. Rev. Lett.* **85**, pp. 3966–3969, 2000.
5. O. F. Siddiqui, M. Mojahedi, and G. V. Eleftheriades, "Periodically loaded transmission line with effective negative refractive index and negative group velocity," *IEEE Trans. Antennas Propagat.* **51**(10), pp. 2619–2625, 2003.
6. M. Notomi, "Theory of light propagation in strongly modulated photonic crystals: Refractionlike behavior in the vicinity of the photonic band gap," *Phys. Rev. B* **62**, p. 10696, 2000.

7. M. S. Wheeler, J. S. Aitchison, and M. Mojahedi, "Negative refraction in a photonic crystal with a metallic cross lattice basis," *Phys. Rev. B* **71**(15), p. 155106, 2005.
8. R. A. Shelby, D. R. Smith, and S. Schultz, "Experimental verification of a negative index of refraction," *Science* **292**, pp. 77–79, 2001.
9. A. Grbic and G. V. Eleftheriades, "Overcoming the diffraction limit with a planar left-handed transmission-line lens," *Phys. Rev. Lett.* **92**(11), p. 117403, 2004.
10. S. O'Brien and J. B. Pendry, "Photonic band-gap effects and magnetic activity in dielectric composites," *J. Phys.: Condens. Matter* **14**, pp. 4035–4044, 2002.
11. K. C. Huang, M. L. Povinelli, and J. D. Joannopoulos, "Negative effective permeability in polaritonic photonic crystals," *Appl. Phys. Lett.* **85**(4), pp. 543–545, 2004.
12. M. S. Wheeler, J. S. Aitchison, and M. Mojahedi, "Magnetism and effective electromagnetic parameters from dielectric spheres," in *Proc. IASTED Antennas, Radar, and Wave Propagat.*, **475**, p. 143, (Banff, Canada), July 2005.
13. C. F. Bohren and D. R. Huffman, *Absorption and Scattering of Light by Small Particles*, Wiley-Interscience, New York, NY, 1983.
14. J. D. Jackson, *Classical Electrodynamics*, John Wiley and Sons Inc., New York, NY, third ed., 1999.
15. W. T. Doyle, "Optical properties of a suspension of metal spheres," *Phys. Rev. B* **39**(14), pp. 9852–9858, 1989.
16. M. Born and E. Wolf, *Principles of Optics: Electromagnetic Theory of Propagation, Interference and Diffraction of Light*, Cambridge University Press, Cambridge, UK, seventh ed., 2002.
17. C. Kittel, *Introduction to Solid State Physics*, John Wiley and Sons Inc., New York, NY, seventh ed., 1996.
18. M. Schall, H. Helm, and S. R. Keiding, "Far infrared properties of electro-optic crytals measure by thz time-domain spectroscopy," *Int. J. Infrared Millimeter Waves* **20**, p. 595, 1999.
19. T. Koschny, P. Markoš, D. R. Smith, and C. M. Soukoulis, "Resonant and antiresonant frequency dependence of the effective parameters of metamaterials," *Phys. Rev. E* **68**, p. 065602(R), 2003.
20. N. Stefanou, V. Yannopapas, and A. Modinos, "Multem 2: A new version of the program for transmission and band-structure calculations of photonic crystals," *Comp. Phys. Comm.* **132**, pp. 189–196, 2000.
21. M. Mojahedi, E. Schamiloglu, F. Hegeler, and K. J. Malloy, "Time-domain detection of superluminal group velocity for single microwave pulses," *Phys. Rev. E* **62**, pp. 5758–5766, 2000.
22. V. Yannopapas and A. Moroz, "Negative refractive index metamaterials from inherently non-magnetic materials for deep infrared to terahertz frequency ranges," *J. Phys.: Condens. Matter* **17**, pp. 3717–3734, 2005.